Accepted Manuscript

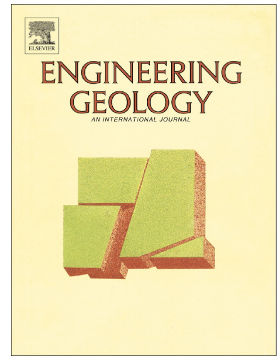

First-time landslides in Vashon advance glaciolacustrine deposits, Puget Lowland, U.S.A.

Thomas C. Badger, Marco D'Ignazio

PII: S0013-7952(18)30621-5
DOI: doi:10.1016/j.enggeo.2018.07.011
Reference: ENGEO 4890

To appear in: *Engineering Geology*

Received date: 17 April 2018
Revised date: 23 June 2018
Accepted date: 9 July 2018

Please cite this article as: Thomas C. Badger, Marco D'Ignazio , First-time landslides in Vashon advance glaciolacustrine deposits, Puget Lowland, U.S.A.. Engeo (2018), doi:10.1016/j.enggeo.2018.07.011

First-time landslides in Vashon advance glaciolacustrine deposits, Puget Lowland, U.S.A.

Corresponding author
Thomas C. Badger
Badger Geotechnics
1802 Pine Avenue NE
Olympia, Washington 98506
USA
BadgerGeotechnics@gmail.com
+1 360 628 6143

Marco D'Ignazio
Norwegian Geotechnical Institute
P.O. Box. 3930 Ullevål Stadion, N-0806
Oslo, Norway
Marco.DIgnazio@ngi.no
+47 922 95 079

Abstract

Advance glaciolacustrine (*Qglv*) deposits from the last continental glaciation are widespread in the densely populated Puget Lowland and are prone to shallow landsliding. Much less frequently in historic time, new landslides propagate deeply within intact *Qglv* deposits. The exceptional volume and highly mobile nature of the 22 March 2014, State Route 530 (Oso) landslide generated considerable uncertainty and public concern about the likelihood for similar deep-seated failures initiating from most any slope where these deposits crop out. The primary study objectives are to utilize geotechnical data from the small data set of available published and public-domain investigations to characterize, in general terms, hydrogeologic, geotechnical and geomorphic factors and their relative contribution to initiating deep-seated landslides within intact *Qglv* deposits; and to inform future hazard and risk assessments for first-time landslides within these deposits.

Qglv deposits are overconsolidated, very stiff to hard, laminated to massive, silt and clay. Shear strength is anisotropic, with cohesion being a significant component of bedding-parallel strength and friction dominating strength perpendicular to bedding. Hydraulic conductivity is likely also anisotropic. Multi-year records of pore pressures within *Qglv* deposits show no to minor seasonal flux; only minor pore pressure responses to multi-day to multi-week episodes of heavy precipitation have been detected. Back analyses using limit-equilibrium methods and peak anisotropic strength under drained conditions demonstrate initial stability of the slopes. Instability occurs near the fully softened strength. We conclude that, over the long term, loss of cohesive strength, rather than hydroclimatic pore pressure response, is the more important contributor to diminishing stability and, in some cases, initiation of first-time landslides in *Qglv* deposits. The shape and location of the slide surface is strongly influenced by strength anisotropy and stress state. Sliding surfaces developed near the basal contact of the *Qglv* deposits in all of the five studied landslides. Higher stress states associated with increasing sequence thickness of the landslide masses decrease stability. The length of the basal slide surface, and thus the aspect ratio of the landslide mass, appears to increase proportionally with sequence thickness of the landslide mass.

Keywords

Overconsolidated clay, anisotropy, pore pressure, Oso landslide, Woodway landslide

1. Introduction

The 22 March 2014, State Route (SR) 530 (herein referred to as Oso) landslide in Washington State resulted in the deaths of 43 people, when a portion of a 200-m-high, glacial fill terrace catastrophically collapsed and ran out more than a kilometer onto the valley floor and inundated a rural residential community. The Oso landslide occurred within deposits of the last major continental glaciation into the Puget Lowland, named the Vashon Stade of the Fraser Glaciation (Armstrong et al., 1965). The basal slide surface developed in the lower portion of the Vashon sequence and mostly within intact advance glaciolacustrine deposits (*Qglv*) (Keaton et al., 2014; Badger, 2015; Pyles et al., 2016). Having been overridden by the kilometer-thick Vashon ice sheet (Thorson, 1980), *Qglv* deposits are characteristically very stiff to hard in consistency, laminated to thinly bedded, nonplastic silt to fat clay (Mullineaux et al., 1965; Landau Associates, 1998; Badger, 2015 and 2016). *Qglv* deposits crop out extensively in marine bluffs and valley slopes in the Cascade and Olympic foothills (Fig. 1). As such large and catastrophic landslides had not occurred elsewhere within these deposits in at least the last century, the event generated considerable uncertainty and public concern about the likelihood for similar style failures initiating from most any slope where these deposits are found.

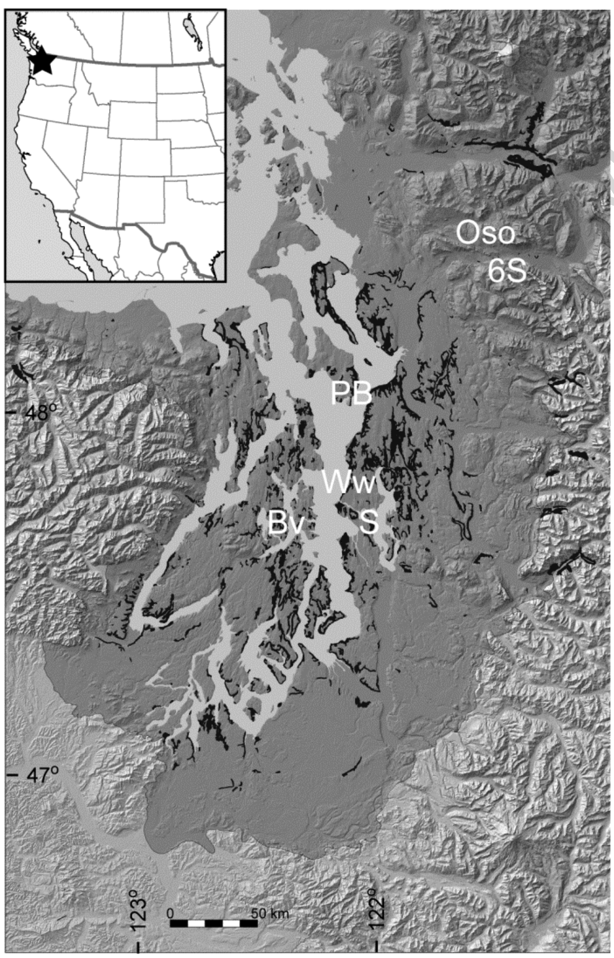

Figure 1. Shaded relief map of Puget Lowlands and southern Salish Sea; Seattle (S) is identified. Landslide sites include Oso, BA6S (6S), Woodway (Ww), Possession Bay (PB), and Brownsville (Bv). Darker gray shading

delimits glacial maximum of Vashon Stade around 17 ka. Black polygons depict exposures of Vashon advance deposits, based on 1:100k geologic map compilations (courtesy of Washington Geological Survey).

During the wet season of October through April, mass wasting is a widespread geomorphic process associated with Vashon glacial deposits. Block falls and shallow debris slides occur frequently on lowland valley slopes and marine bluffs. Additionally, *Qglv* deposits commonly perch groundwater and induce landsliding within the overlying advance outwash deposits (Tubbs, 1975). Accumulated fine-grained colluvium on and at the base of these slopes is especially susceptible to precipitation-induced landsliding. Much less frequently in historic time (about one per decade in the last 40 years), new landslides propagate deeply within intact *Qglv* deposits (Laprade et al., 1998). The 1997 Woodway landslide just north of Seattle (Laprade et al., 1998; Arndt, 1999) and the large retrogression associated with the Oso landslide are examples of such failures.

Landslides initiating within previously unsheared earthen materials are commonly termed *first-time landslides* (Skempton and Hutchinson, 1969). Deep-seated, first-time landslides within large Puget Lowland slopes, say exceeding 50 m in height and where *Qglv* deposits are present in the lower portion of the slope, have involved debris volumes ranging from tens of thousands to tens of millions of cubic meters. Some of these collapsed catastrophically and subsequently became highly mobile. More commonly, large steep slopes with *Qglv* deposits within the Vashon stratigraphic sequence have been demonstrably stable for decades to perhaps centuries or millennia.

The correlation of extended and/or intense periods of precipitation with elevated pore pressure is a widely known trigger of landslide initiation in many geologic settings and materials, as well as certain failure modes. Given the reported and expectedly low hydraulic conductivities of intact *Qglv* deposits (Galster and Laprade, 1991; Morgan and Jones, 1995), it is intuitively unclear to what extent hydroclimatic conditions could influence pore pressures within a few days to weeks, or even seasonally. This rainfall-initiation connection would seem to have even greater uncertainty in glacial sequences in the Puget Lowlands, where *Qglv* deposits commonly underlie till aquitards and unsaturated zones that impede downward flow and recharge. Further, the horizontally laminated to thinly interbedded nature of glaciolacustrine fine sands, silts and clays would be expected to have contrasting vertical and horizontal conductivities, favoring horizontal rather than vertical groundwater flow and recharge. Such anisotropy in hydraulic conductivity has been documented in similar deposits in the Northern Hemisphere (i.e., Nieuwenhuis and Van Genuchten, 1986; La Meil, 2017). Also of curiosity is the first-time, large-volume 1979 Possession Bay landslide on Whidbey Island, which apparently involved intact *Qglv* deposits and moved during the summer dry season (Arndt, 1999). These inferences complicate the conventional application of precipitation's important short to intermediate-term role on landslide initiation for the case of first-time landslides within intact *Qglv* deposits.

Shear strength and stress state deserve consideration, as well, for their roles in long-term stability of slopes partially composed of *Qglv* deposits. Once exposed, overconsolidated silts and clays are well known to experience strength loss through a complex time-dependent process of strain localization, creep, and progressive formation of a slide surface, which is then often followed by a phase of rapid strength loss and failure (i.e., Skempton, 1964; Bjerrum, 1967; Carey and Petley, 2014). Given the horizontally bedded nature and compositional variation within the deposits, their shear strength cannot be isotropic. Intuitively, slide surfaces propagating steeply across bedding, such as along the back scarp, will mobilize higher strength than the basal portion of the slide surface where it should preferentially propagate subhorizontally through weaker layers. In consolidated-drained direct shear tests of overconsolidated glaciolacustrine deposits in northwestern Alberta, Cruden et al. (1997) noted considerably higher strength across bedding when compared to tests conducted parallel to bedding. Comparable results have been noted in similar deposits in Europe (i.e, Giraud et al. 1991; Florkiewicz et al., 2015). This strength anisotropy should influence the configuration and location of the slide surface and landslide type. Stratigraphy and sequence thickness (slope height) should similarly influence stress state within *Qglv* deposits and, thus, slope stability. This was also of interest to Perkins et al. (2017) in their investigation of landslide mobility and the correlation of stratigraphy with the potential source volume of deep-seated landslides occurring in glacial sequences in the Puget Lowland.

The primary objectives of this paper are to:

– Utilize geotechnical data of *Qglv* deposits from available published and public-domain investigations to characterize, in general terms, hydrogeologic, geotechnical and geomorphic factors and their relative contribution to initiating deep-seated landslides within intact *Qglv* deposits; and
– Inform future hazard and risk assessments for first-time landslides within these deposits.

Constrained by the historic infrequency of these first-time landslides, this paper draws from a small data set of five landslides, four historic (since ca 1970s) and one prehistoric, involving large slopes ranging in height from 50 to nearly 200 meters, where *Qglv* deposits have been identified in the mid to lower portions of the slopes (Table 1). Three of these landslides have limited to extensive geotechnical and subsurface data, while no subsurface data exist for the other two. We examine reconnaissance observations, hydroclimatic pore-pressure response, and laboratory test data from various geotechnical investigations. The Oso landslide has, by far, the most detailed characterization of geologic, hydrogeologic and geotechnical conditions, so by necessity we have drawn heavily from these data. Given the varied sediment provenance, mixing during glacial transport and large depositional area, we assume that material properties of *Qglv* deposits throughout the region primarily fall within the range of values measured from the available laboratory testing and back-analyses. Under presumed drained conditions prior to the onset of rapid movement, we perform limit-equilibrium stability analyses to evaluate the influence that pore pressures, strength anisotropy and loss, and stress state may have on the development and configuration of a failure surface.

Table 1. Landslide study sites

Landslide	Occurrence	Location	Subsurface Characterization	References
Possession Bay	1-Jul-1979	Whidbey Island	unknown	Arndt, 1999
Brownsville	1983	Kitsap County	unknown	Arndt, 1999
Woodway	15-Jan-1997	Snohomish County	limited	Landau Associates, 1998; Arndt, 1999; Savage et al., 2000b
Oso	22-Mar-2014	N Fk Stillaguamish	extensive	Keaton et al., 2014; Riemer et al., 2015; Badger, 2015; Badger, 2016; Pyles et al., 2016; Stark et al., 2017
BA6S	prehistoric	N Fk Stillaguamish	limited	Badger, 2015

2. Setting

Proximity to the central Pacific Ocean produces the region's maritime climate, defined by mild wet winters and dry summers. Average annual precipitation in the lowland, falling primarily as rain between November and April, ranges from 500 to 1500 mm near sea level and 1500 to nearly 3000 mm (Western Regional Climate Center) in the surrounding foothills ~300 m in elevation, roughly the elevational extent of the Vashon advance glaciolacustrine deposits.

The Puget Lowland is an active tectonic basin in western Washington State, bounded to the west and east by the mountainous provinces of the Olympic Peninsula and North Cascades, respectively. While Mesozoic and Cenozoic rocks crop out in portions of the central and northern lowland, the basin is extensively filled with unconsolidated Pleistocene glacial and nonglacial deposits, which underlie most of the land surface (Booth, 1994). The Salish Sea occupies the basin and is bound by several thousand kilometers of island and mainland shoreline in Washington State. Much of the shoreline is comprised of moderately steep to near vertical, vegetated to eroding slopes and bluffs rising in excess of 100 m. Many small and large rivers that drain the lowland and bounding mountains have dissected the thick lowland fill, producing valley slopes in the unconsolidated deposits upwards of 300 m in elevation.

Multiple Pleistocene glaciations of both alpine and continental origin have extensively shaped the region and lowland topography. The last major continental glaciation, named the Vashon Stade of the Fraser Glaciation, advanced from British Columbia into the Puget Lowland around 18 ka (Armstrong et al., 1965; Porter and Swanson, 1998). Proglacial lakes formed in closed basins and ice-dammed valleys on the margins of the advancing ice front and rapidly received deposits of fine sand, silt and clay. These advance glaciolacustrine deposits were subsequently buried by fluvial outwash sand and gravel. Inundation by the ice front commonly deposited a capping silt/clay-rich diamict of till on the advance sequence of lacustrine and outwash deposits. Maximum ice thickness of the Puget Lobe may have exceeded 2000 m in the northern Puget Lowland and 1500 m in the vicinity of Seattle (Thorson, 1980). The Puget Lobe reached its southern extent near Olympia ca 13 ka, and then rapidly retreated from the Puget Lowland by 11 ka, leaving behind extensive recessional lacustrine and outwash deposits. The presence and thicknesses of these advance and recessional units can be locally quite variable.

Mullineaux et al. (1965) described the generalized stratigraphy in the Seattle area associated with the onset of the Vashon Stade and assigned the local member name of Lawton Clay for the advance clay and silt beds (glaciolacustrine) at or near the base of the Vashon sequence. In the central Puget Lowland, coarser transitional sand and silt beds commonly bound the basal and upper contacts of the glaciolacustrine deposits with the nonglacial deposits and outwash, respectively. Minard (1982) collectively referred to both the glaciolacustrine and, where present, the upper and lower transitional deposits as the Transitional Beds, which we identify as *Qglv* deposits.

3. Geotechnical Properties

The Vashon advance glaciolacustrine deposits are characteristically massive to laminated nonplastic silts and lean to fat clays with occasional fine sand laminae. The clay fraction primarily consists of chlorite, illite and smectite (Gault, 2015). In the Seattle area, *Qglv* deposits typically have less than 50 m of sediment cover and are described as fissured with some slickensides (Mullineaux et al., 1965; Galster and Laprade, 1991). In the North Fork Stillaguamish valley, the site of the Oso landslide and others, the Vashon sequence is 180 m thick. There, *Qglv* deposits, which constitute the lower half of the sequence, are fissured only in their upper portion; fissures and slickensides are largely absent within the lower portion of the unit.

Standard penetration tests (ASTM D1586) find consistencies that are very stiff to hard (Landau Assoc., 1998; Galster and Laprade, 1991; Badger, 2015 and 2016). Index properties established from laboratory testing are presented in Table 2 (Landau Assoc., 1998; Riemer et al., 2015; Badger, 2016; GeoTesting Express, 2016). From the range of liquidity indices, soil behavior when sheared would primarily be plastic with some samples indicating brittle and slightly sensitive behavior (Holtz et al., 2011). Savage et al. (2000a) reported hydraulic conductivities of *Qglv* deposits in the Seattle area ranging from 10^{-4} to 10^{-9} cm/s. Morgan and Jones (1995) estimated the ratio of horizontal to vertical conductivities for advance sand and silt deposits to be 100 to 200; we expect similar or higher ratios for *Qglv* deposits.

Table 2. Geotechnical index properties of *Qglv* deposits

Landslide	# of Samples	Moisture Content (%)*	Bulk Density (kg/m^3)*	SpG*	LL*	PL*	PI*	LI*	Clay Content (%)*	Soil Classification	Reference
Oso	6	26-36 (30)	1870-1990 (1940)	2.77-2.81 (2.79)	48-70 (59)	24-26 (25)	23-45 (34)	-0.6-0.4 (0.1)	35-66 (47)	CL-CH	Riemer et al., 2015
Oso	14	24-42 (31)	1860-2010 (1940)	2.68-2.79 (2.74)	27-67 (49)	19-28 (22)	8-43 (27)	0.1-2.3 (0.4)	12-52 (27)	CL-CH	GeoTesting Express, 2016
Oso	78	12-41 (30)	1860-2160 (2020)	2.61-2.87 (2.78)	22-59 (44)	NP-31 (26)	NA-31 (19)	-1.7-2.0 (0.1)	16-52 (29)	ML-MH-CL-CH	Badger, 2016
Woodway	7	23-41 (30)			34-72 (41)	24-36 (25)	11-37 (17)	0-0.7 (0.3)		ML-MH	Landau Associates, 1998

*Value range (mean)

In his review of available consolidation test data for *Qglv* deposits in the Seattle area, Laprade (1982) found no apparent correlation of preconsolidation pressures with burial depth. A correlation of preconsolidation pressure and burial depth was apparent, however, for samples proximal to high-conductivity stratigraphic units. Constant-strain-rate consolidation tests performed on relatively undisturbed tube samples from the Oso landslide yielded a range of maximum preconsolidation pressures of 1200 to 3600 kPa and overconsolidation ratios (OCR) ranging from 1 to 1.2 for recently exhumed *Qglv* deposits located below the new slide surface (Pyles et al., 2016; Riemer, 2016). Stark et al. (2017) performed three consolidation tests for the Oso landslide on block samples taken from the landslide debris, which yielded a maximum preconsolidation pressure of 1628 kPa and OCRs ranging from 4 to 8.

Few published or public-domain geotechnical investigations exist that include shear-strength characterization of intact *Qglv* deposits through laboratory testing and/or back-analysis of failure. These include the landslides that occurred during construction of the Seattle Freeway in the 1960s (Palladino and Peck, 1972); the 1997 Woodway landslide (Landau, 1998; Arndt, 1999; Savage et al., 2000a,b); and the Oso landslide (Badger, 2016; Pyles et al., 2016; Cooper Testing Laboratory, 2016; GeoTesting Express, 2016; Stark et al., 2017). Anisotropic strengths were investigated for the Oso landslide using consolidated-drained direct shear testing (ASTM D3080) and shearing samples parallel to bedding (Badger, 2016; Cooper Testing Laboratory, 2016; GeoTesting Express, 2016) and perpendicular to bedding (Badger, 2016); failure envelopes are presented in Figures 2a and b, respectively. Typical stress-strain curves from the direct shear tests indicate brittle behavior with significant strain softening to plastic behavior and minor strain hardening; peak strength is commonly reached between 3 and 7% strain. Torsional ring shear tests were performed to assess strengths for fully-softened (ASTM D7608) and residual states (ASTM D6467) for the Oso landslide (Badger, 2016; Cooper Testing Laboratory, 2016; Stark et al., 2017). These data are summarized in Table 3.

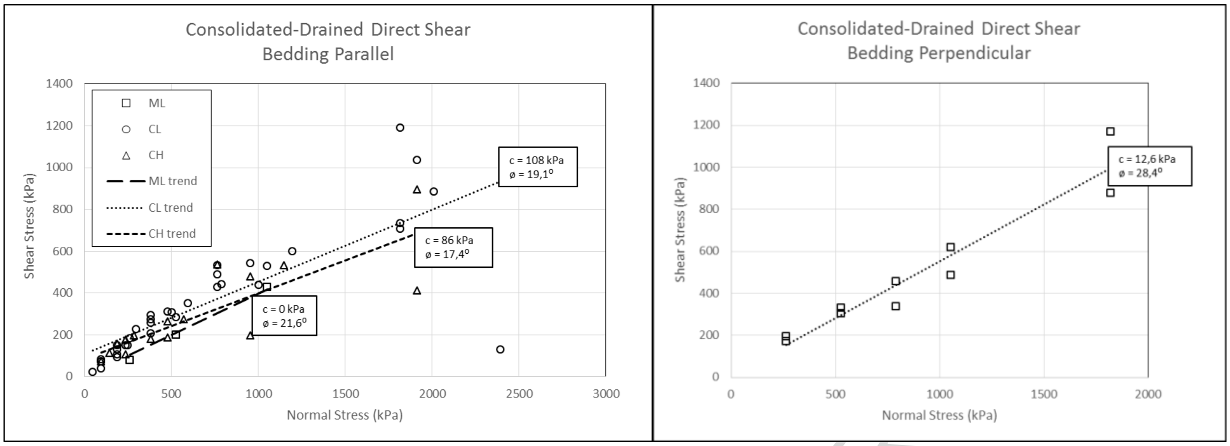

Figure 2. Peak drained strength envelopes from direct shear tests on samples sheared a) parallel to bedding and b) perpendicular to bedding.

Table 3. Shear strength of *Qglv* deposits

Reference	Peak Isotropic		Peak Anisotropic-Parallel		Peak Anisotropic-Perpendicular		Fully Softened	Residual
	cohesion (kPa)	friction	cohesion (kPa)	friction	cohesion (kPa)	friction		
Palladino & Peck, 1972	62	35°	-	-	-	-	-	13.5-17.5°
Arndt, 1999			-	-	-	-	-	
- ML (upper)	0	25°	-	-	-	-	-	22-24°
- CL/CH (lower)	0-38	15-27°	-	-	-	-		6-27°
Savage et al., 2000a	12	24°	-	-	-	-	-	-
Pyles et al., 2016	5-10	20°	-	-	-	-	20°	12°
Badger, 2016	-	-			12.6	28.4°		12-22°
- ML			0	21.6°				11.7-13.3° *
- CL			108	19.1°				20.4-22.2°
- CH			86	17.4°			22.8-23.2°	15.1-18.8°
Stark et al., 2017	-	-	-	-	-	-		
- ML/CL							25-34°	20-27°
- CH							21-32°	12-19°

* Torsional ring shear results for residual strength of dark gray, organic-rich silt

4. Role of Precipitation

To examine the role precipitation may have on landslide initiation within intact *Qglv* deposits, we synthesized available hydrogeologic and hydroclimatic data for three first-time landslides. We introduce this topic, however, with description of a fourth large-volume landslide that occurred during the summer dry season, for which only surficial characterization exists.

4.1 Possession Bay Landslide

In his evaluation of landslides occurring within similar intact sequences of Vashon glacial deposits as the Woodway landslide, Arndt (1999) reported on a large landslide in an 80-m-high marine bluff on the southeast end of Whidbey Island, south of the community of Glendale (Fig.

3a). The landslide, which exhibited considerable mobility, occurred on 1 July 1979 during the summer dry season and following four months of below-normal precipitation. Minard (1982) included the landslide in his regional geologic mapping, and identified the bluff sequence as Vashon till, advance outwash and transitional beds (*Qglv* deposits) overlying PreVashon interglacial deposits (Whidbey Formation). Arndt's interpreted section of the landslide, prepared nearly 20 years after the event, is presented in Figure 3b; we attempted to assign Minard's geologic units to Arndt's section. The failure surface is depicted as shearing deeply through the Vashon sequence, possibly extending into the underlying PreVashon deposits. A slope inflection evident in the lower third of the landslide scar and the absence of a debris bulge or accumulation at the base of the slope suggest the failure surface is well above beach level. No borings or instrumentation data are available for this landslide to confirm stratigraphy and groundwater conditions behind the landslide, or the location of the basal failure surface. The reason for including this feature is to note that we consider it improbable that precipitation-induced pore pressures developed during the preceding four months to cause this movement.

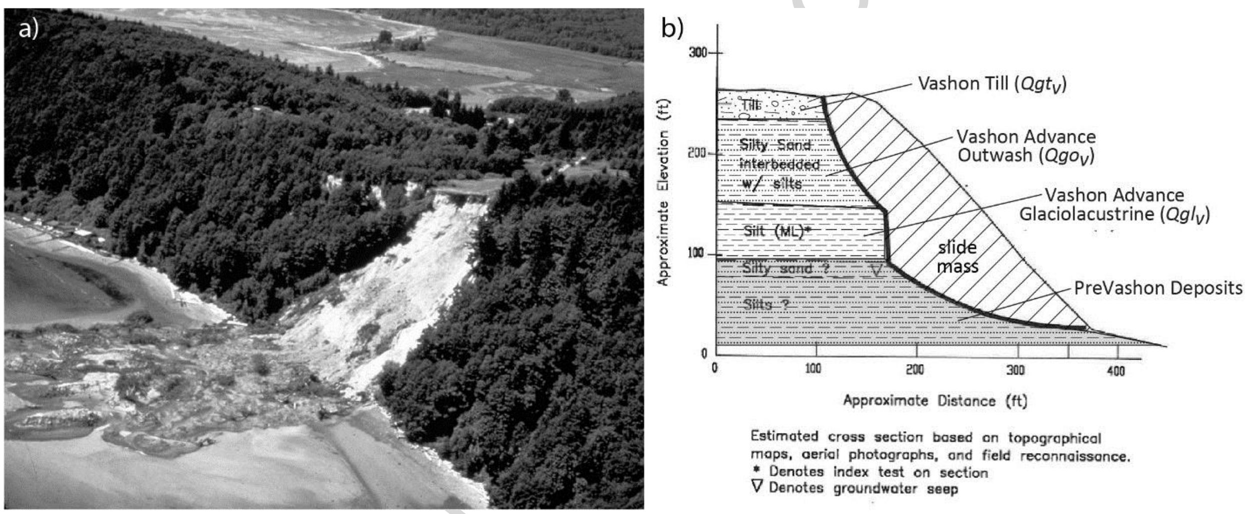

Figure 3. a) Photo of 1 July 1979 Possession Bay landslide (courtesy of D. Frank and H. Shipman). b) Measured geologic section (courtesy of Arndt, 1999), with interpreted geologic units based on regional mapping of Minard (1982).

4.2 Woodway Landslide

On 15 January 1997, a rapid landslide initiated from a steep 75-m-high marine bluff located near the community of Woodway, about 25 km north of downtown Seattle (Fig.4). The landslide followed more than a year of above-normal precipitation; then several weeks prior to the event, a series of winter storms brought more with than 50 cm of snowfall that was followed by warm heavy rains (Gerstel et al., 1997). Estimated to involve 100,000 m^3 of intact Vashon advance glacial deposits, it *"...probably represent[ed] one of the larger coastal bluff landslides to have occurred in the last 30 years or so"* (Landau Assoc., 1998).

Figure 4. Photo of 15 January 1997 Woodway landslide (courtesy of H. Shipman).

Landau performed a geotechnical investigation, including borings and piezometers, to characterize the stratigraphic and groundwater conditions in the bluff immediately behind the head scarp (Fig. 5). The landslide failed through a discontinuous 4-m cap of very dense diamict (till), about 25 m of advance outwash sand and interbedded silt, and ~20 m of fractured (fissured) advance glaciolacustrine silt and clay (*Qglv*). The surface rupture toe was interpreted to be near or just below the contact of the *Qglv* unit and PreVashon interglacial deposits (Whidbey Formation), consisting of very dense sand with interbedded hard sandy to clayey silt. Post-failure observations included many iron-stained fractures within landslide blocks of glaciolacustrine deposits and seepage within the back scarp from fractures within the advance glaciolacustrine deposits (Laprade et al., 1998). These observations suggest that groundwater flow and likely rapid recharge were dominated by fractures rather than interstitial pores. Landau inferred that above-normal precipitation preceding the failure, and resultant elevated pore pressures facilitated by the pre-existing tension cracks and fractures, were the primary controls on this failure.

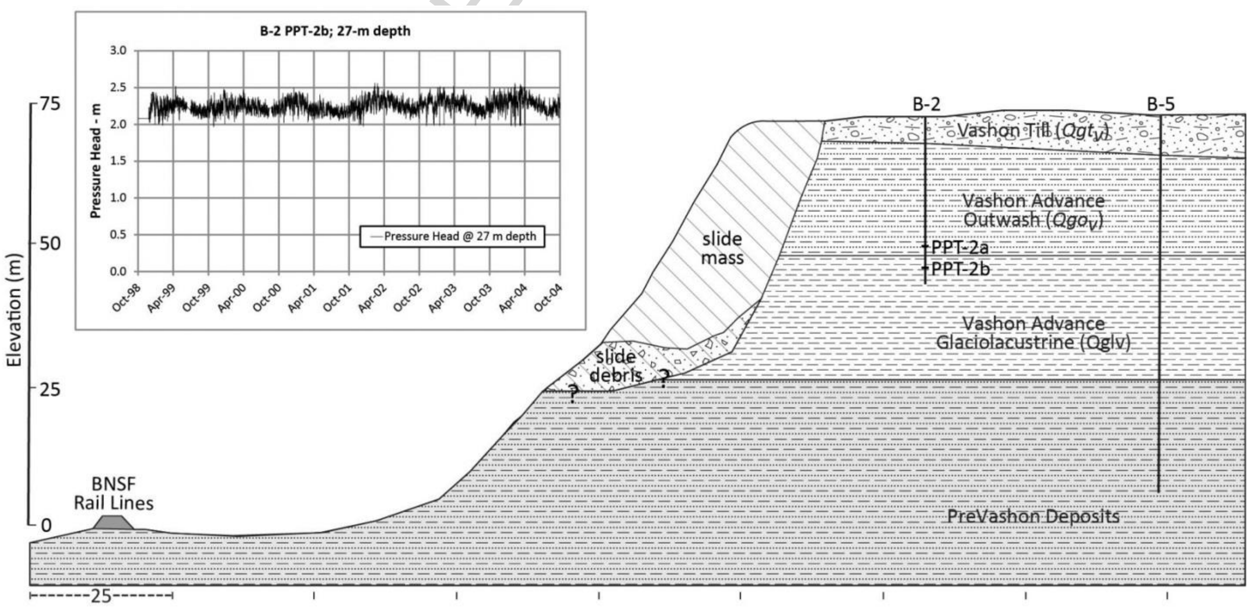

Figure 5. Geologic section of Woodway landslide (modified from Landau Assoc., 1998). Graph depicts pressure head on vibrating-wire piezometer PPT-2b at 27 m depth from boring B-2, located in the upper portion of the Vashon glaciolacustrine deposits for 1998 through 2003 water years. Unsaturated conditions were measured in the overlying outwash unit (PPT-2a) during this 6-yr period.

One sanded-in-place, vibrating wire piezometer was installed in July 1997 near the top of the advance glaciolacustrine unit (PPT-2b), about 3 m below the contact with advance outwash. The piezometer (and other on-site instrumentation) was continuously monitored at 15-min intervals by the U.S. Geological Survey until 2005 (Fig. 5) (USGS, 2006). The presented data spans six water years beginning in October 1998 through September 2004. The on-site precipitation record is incomplete for this period and is not included, though typical seasonal quantities and patterns of dry summers and wet winters persisted during this monitoring period (Western Regional Climate Center). An annual fluctuation of about 0.3 m of pressure head was measured during this 6-yr period, with heads gradually increasing and peaking in late winter, then gradually dropping with the onset of the dry summer season. We recognize no indication in these data of response to significant storms during this period.

4.3 Oso Landslide

4.3.1 Background

Since at least the 1930s, landslide debris thickly mantling this valley slope in the North Fork Stillaguamish River valley experienced occasional wet-season remobilizations (usually called the Hazel slide, in pre-2014 literature; Shannon, 1952; Thorsen, 1970; Benda et al., 1988; Miller and Miller, 1999). The penultimate remobilization occurred in January 2006 and involved between 1 and 2 million m^3 of landslide debris (Badger, 2015). Much of it fluidized and rapidly ran out nearly 250 m onto the valley floor, temporarily damming and diverting the river. That event was unnoticed by a nearby fisherman (Stillaguamish Tribe, 2006) and was unrecognizable in a review of the regional seismic network records (K. Allstadt, 2014 personal communication; Iverson et al., 2015). Initiating from this same slope, the catastrophic 2014 Oso landslide (Fig. 6) followed a multi-week period of heavy rains. This landslide originated within the 200-m-high glacial-fill terrace, retrogressing nearly 100 m into the intact sequence of glacial deposits composing the terrace. It evolved rapidly into a highly mobile debris avalanche-debris flow that reached the opposite valley wall more than a kilometer away in about a minute (Keaton et al., 2014; Iverson et al., 2015).

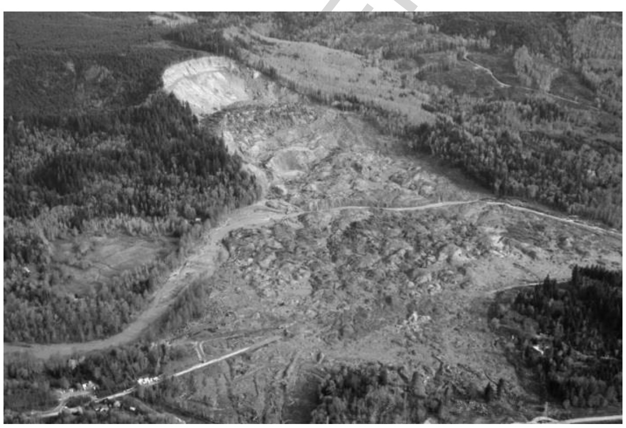

Figure 6. Photo of 22 March 2014 Oso landslide (courtesy of the Washington State Patrol).

Geotechnical borings in the terrace behind the head scarp in 2014 and in the landslide body in 2015 (Badger, 2015, 2016), along with surface topography from lidar surveys in 2003, 2013 and 2014, form the basis of our interpreted geologic section through the landslide mass (Fig. 7). Based on near-continuous samples recovered in the 2015 borings, we interpret the basal slide surface to be located almost entirely within the *Qglv* deposits. The slide surface is about 400 m in length and dips gently for much of its length about 2°. The back scarp is arcuate and steep, and the central slide mass comprises large, back-rotated blocks (Keaton et al., 2014) rooted on a nearly planar basal failure surface. Using classification schemes of Skempton and Hutchinson (1969) and Hungr et al. (2014), the initiating landslide mass would be classified as a compound slide. The landslide volume is approximately 10.1 million m^3, based on a three-dimensional subsurface model derived from the 2015 borings, (B. Collins, 2018, personal communication). Approximately 70% of the 2014 landslide volume was intact, comparatively strong, Vashon-age glacial deposits; the outer mantle of comparatively weak, prehistoric and historic landslide deposits made up just 30% of the mass. The interpreted geologic sections of Stark et al. (2017, their Figs. 9 and 13) depict the basal failure surface 20 to 30 m higher than indicated by the 2015 borings, and we believe underrepresent the actual landslide volume by ~25%.

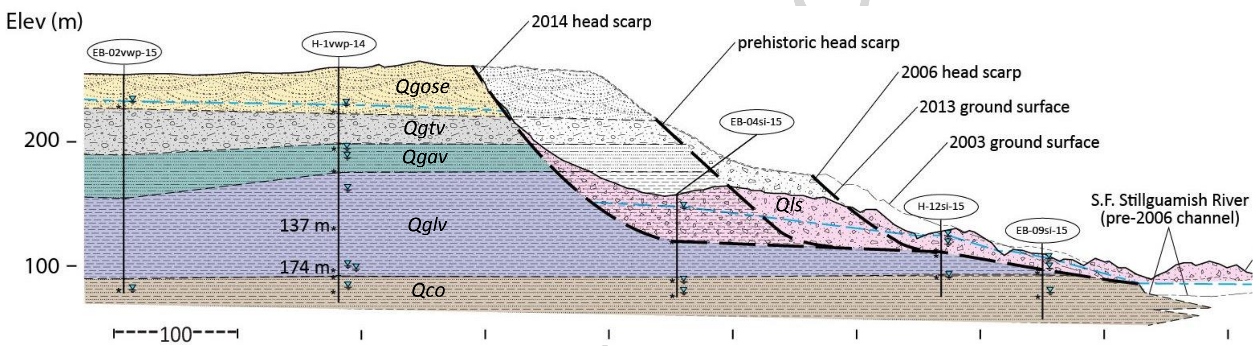

Figure 7. Interpreted geologic section of the Oso landslide, based on 2014 and 2015 geotechnical borings (need key/legend to explain symbols). Stratigraphic symbols include landslide debris (*Qls*), recessional outwash (*Qgose*), Vashon till (*Qgtv*), Vashon advance outwash (*Qgav*), Vashon advance glaciolacustrine (*Qglv*), and Vashon (?) advance deltaic sand (*Qco*). Asterisks left of borings are vibrating wire piezometers and corresponding maximum pressure head (right side).(color)

Many investigators of the 2014 Oso landslide (Keaton et al., 2014; Iverson et al., 2015; Wartman et al., 2016; Pyles, et al., 2016; Stark et al., 2017) have inferred that above-average rainfall over the preceding weeks was an important causal factor for this event. They further deduced that movement began with the mobilization of the saturated and mantling landslide debris and then retrogressed into the intact glacial sequence. To reexamine these interpretations and the potential contribution of precipitation, we first review eyewitness accounts and published analyses of seismic data at the onset of failure.

4.3.2 Initiation Sequence

Unlike the 2006 landslide, nearly a dozen eyewitnesses reported very loud noises accompanying the 2014 landslide, which have been grouped into two phases (Badger, 2015; Iverson et al., 2015; Pyles et al., 2016). The first phase of noise preceded the catastrophic collapse of the slope, which we have estimated to have been between 50 and 70 s in duration. After a brief cessation of noise, the slope collapsed and an extremely rapid torrent of debris inundated the valley; this collapse and runout is associated with the second phase of noise.

Also unlike the 2006 event, landslide motion was detected by at least eighteen stations in the regional seismic network, identifiable as two distinct pulses of seismic energy separated by a brief period of quiescence. Iverson et al. (2015) and Hibert et al. (2014) both found that the initial phase of landslide motion, about 50 seconds in duration, generated only long-period seismic energy, "…*indicative of acceleration of a relatively coherent mass of material.*" The second phase was dominated by high frequency (short period) seismic energy that was attributed to significant acceleration of the landslide mass and "*highly agitated*" movement.

In the context of the geologic section, we believe that the eyewitness account and seismologic analyses support an alternative initiation sequence. There seems to be widespread agreement that much of the 2014 slide mass comprises a series of rotational blocks. Retrogression into the glacial terrace through a rotational failure mode required the formation of a new slide surface. Shearing of intact material occurred along the entire length of the base of the block and back scarp, a length of about 350 m. The initial phase of long-period motion and first phase of noise, corresponding to failure of a "*relatively coherent mass*", would therefore seem to be more appropriately attributed to slope movement within this comparatively strong intact sequence, constituting 70% of the 2014 slide mass. The remaining 30% that mantled the slope was weaker, dilated, wet, and frequently remobilized landslide debris at the base of the slope. We think the second phase of noise and seismic energy would then be associated with the rapid collapse and dispersal of debris. While the buttressing effect of the landslide debris is substantial for the entire 2014 landslide mass, instability of the upslope intact mass can be achieved without prior movement of the landslide debris and is discussed in Section 5.1.

This alternate scenario of the 2014 event initiating within the intact sequence of glacial deposits would, by spatial necessity, entail shoving the weak, wet landslide deposits at the base of the slope ahead of the large disaggregating mass of intact glacial deposits following closely behind. If this failure scenario is valid, it raises questions about what influence precipitation could have had on pore pressures within the low-conductivity, glaciolacustrine deposits, where most of the failure surface developed.

4.3.3 Hydroclimatic Pore Pressure Response

Borings and instrumentation allow identification of varied hydrogeologic conditions in the terrace behind the 2014 head scarp from the ground surface to below river level (Fig. 7):

- a perched aquifer within recessional outwash sands and silts (*Qgose*);
- a thick aquitard of compact lodgment till, primarily clay-rich diamict (*Qgtv*);
- a thin unsaturated zone beneath the till in advance outwash sands and silts (*Qgav*), becoming saturated and likely perching on the underlying advance glaciolacustrine silt and clays;
- mostly to fully saturated glaciolacustrine silts and clays (*Qglv*), and
- a basal unit at river level of glacial or interglacial fluvial/deltaic sands (*Qco*), the upper portion of which may be unsaturated.

Because of the two unsaturated zones and thick aquitard that overlie the glaciolacustrine unit, we expect that recharge and pore pressure response is dominated by horizontal conductivity within the *Qglv* unit, involving water from outside the immediate area of the landslide.

Seven grouted-in-place, vibrating wire piezometers were installed in November 2014 within this intact glacial sequence about 100 m behind the 2014 head scarp, including two within the *Qglv* unit at 137 m and 174 m depths (Fig. 7). A nearly 4-yr record of precipitation and pore pressure data from these two piezometers continuously collected at 2-hr intervals are presented in Figures 8a and b, respectively. These piezometers took nearly a year to equilibrate and hydraulically connect with the formation. For the 2015 through 2017 water years, positive pressure response coincided closely with the typical onset of October rains; pressures peaked at the end of the wet seasons with up to 1.2 to 1.6 m of seasonal head flux, after which pressures dissipated with drier seasonal conditions. Evident, as well, is much lower pore pressure at the base of the *Qglv* unit, and possibly localized unsaturated conditions where it overlies a more conductive sand unit.

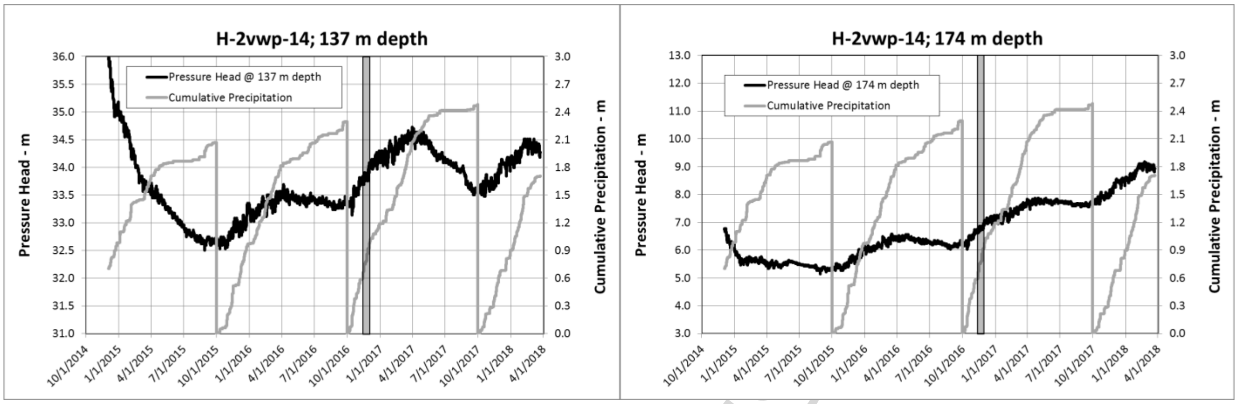

Figure 8. Cumulative precipitation and piezometer data, plotted as pressure head above instrument, from the Oso landslide at depths of a) 137 m and b) 174 m, for 2014 through most of 2017 water years. Shaded columns delineate 21-day period (depicted in greater detail in Figures 9a and b) during which time 400 mm of precipitation was recorded at the site.

The contribution from storms and shorter-duration wet periods on pore pressures within *Qglv* deposits has also been an unanswered question. Henn et al. (2015) estimated that between 300 to 400 mm of rain fell on the site in the 21 days preceding the 22 March 2014 landslide event. Serendipitously, an on-site rain gage installed post-failure recorded 400 mm of rainfall during a 21-day period between 12 November and 3 December 2016. Rises of ~0.4 m of pressure head were recorded at the end of and shortly following this 21-day period (Figs. 9a, b). If recharge is dominated by horizontal flow along bedding, pore pressure response from the preceding weeks of heavy rainfall before the March 2014 landslide should not be substantially different than the 21-day wet period in November-December 2016.

We conclude, then, that the weeks of heavy rains that preceded the 2014 landslide did not induce a spike in pore pressures that resulted in significant strength loss within the intact *Qglv* deposits. However, as the measured pressure responses were greater for seasonal inputs than those from storms, and recalling that the 2014 landslide occurred near the time of wet-season maximum, we infer that seasonal precipitation could have had a slight destabilizing influence within the intact mass of *Qglv* deposits at Oso. It is also possible that the preceding four water years of above-average precipitation induced higher pore pressures than have been detected in the four water years of post-landslide piezometer data. The possible interactions of seasonal and storm precipitation in these events is discussed in Section 4.5.

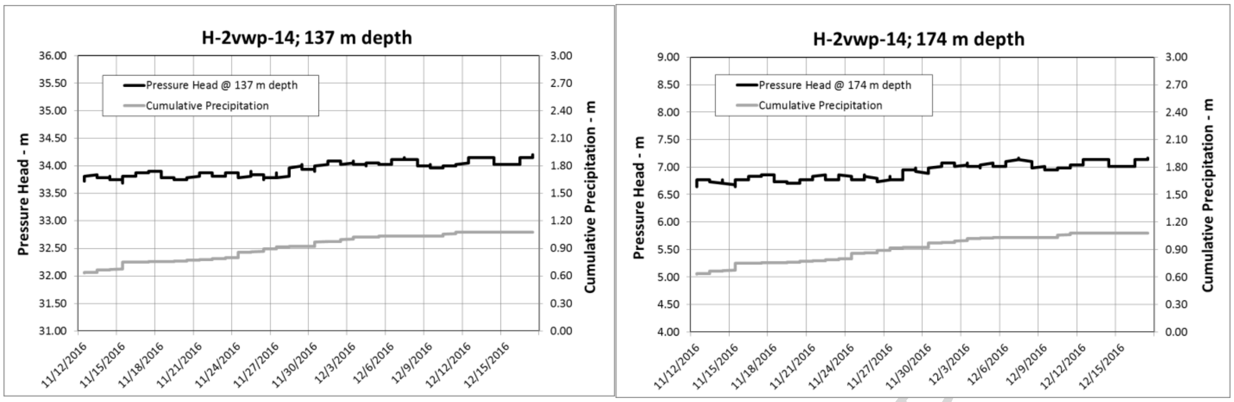

Figure 9. Cumulative precipitation and piezometer data, plotted as pressure head above instrument, from the Oso landslide at depths of a) 137 m and b) 174 m, for a 21-day period, when 400 mm of rain fell between 12 November and 3 December 2016.

4.4 BA6S Landslide

Directly across from the Oso landslide in the North Fork Stillaguamish River valley is a large prehistoric landslide, referred to as BA6S (Gerstel and Badger, 2014), which moved north from the opposite glacial-fill terrace (Fig. 10). Like the Oso landslide, debris from the BA6S landslide was transported at least one kilometer from the depletion zone; the distal deposits have been truncated by river erosion. The uniformity of the landslide deposits and head scarp, coupled with comparably large depletion and accumulation volumes, suggest that this landslide may have failed as a single event involving more than 40 million m^3 of intact glacial deposits (Badger, 2015). We compiled a geologic section (Fig. 10) through the landslide from mapping by Dragovich et al. (2003) and two geotechnical borings drilled in 2014 (Badger, 2015). The basal failure surface is located within the lower portion of the *Qglv* unit, and is interpreted to be planar and dipping less than 5°. As at the Oso landslide, the *Qglv* unit overlies glacial or interglacial fluvial and deltaic sands (*Qco*).

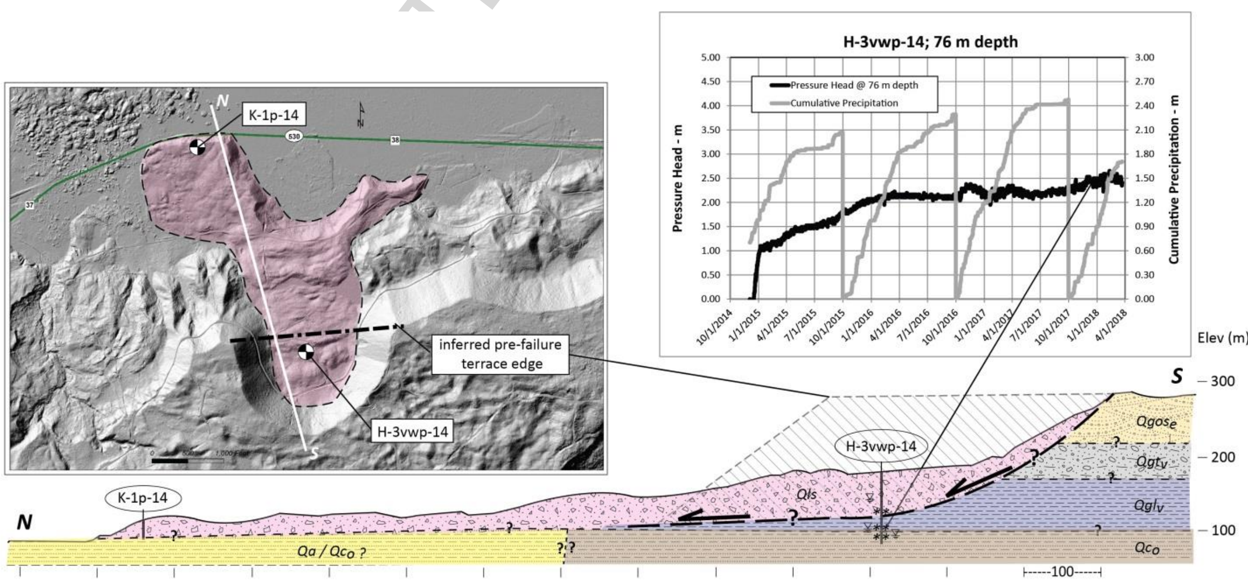

Figure 10. Bare-earth image from 2014 lidar data of prehistoric BA6S landslide and its deposits (pink shading), located immediately south and across the valley from the Oso landslide, the debris from which is evident in upper left corner. Line depicts location of interpreted geologic section shown in the cross-section. Stratigraphic symbols

include landslide debris (Qls), recessional outwash (Qgose), Vashon till (Qgtv), Vashon advance glaciolacustrine (Qglv), and Vashon(?) advance deltaic sand (Qco). Asterisks along upslope boring are vibrating wire piezometers and corresponding maximum pressure head. Graph presents cumulative precipitation and pressure head on vibrating-wire piezometer, located near the base of the *Qglv* unit, collected during 2014 through most of 2017 water years. (color)

Three grouted-in-place, vibrating wire piezometers were installed in the 2014 boring, including one just beneath the failure surface within intact *Qglv* deposits at 76 m depths. A nearly 4-yr record of this piezometer along with precipitation continuously collected at 2-hr intervals is presented in Figure 10. The piezometer took about two years to equilibrate and hydraulically connect with the formation. For the 2016 and 2017 water years, pore pressure was quite low, and there was no or only minimal (<0.3 m) pressure response to the wet season or shorter durations of heavy rain.

4.5 Discussion

Available pore pressure data indicate that all vibrating wire piezometers eventually gained hydraulic connection with the low-conductivity glaciolacustrine formation and subsequently measured positive pore pressures, indicating saturated conditions. Further, all instruments measured pressure change, albeit minor, over an annual cycle with an expected wet-season increase and dry-season decrease; barometric pressure response was also evident. Where low-conductivity *Qglv* deposits overlie higher-conductivity sand deposits at the Oso and BA6S landslides, low pore pressures were measured in the *Qglv* deposits near the contact. This relationship between stratigraphy and pore pressures was also observed in landslides that occurred within *Qglv* deposits encountered in excavations for the Seattle Freeway (Palladino and Peck, 1972). We attribute this zone of low pore pressure to vertical drainage into the underlying sand unit due to a conductivity gradient between units. High effective normal stresses in the lower portion of the *Qglv* unit would result and actuate additional shear strength near the stratigraphic contact. This may explain why the failure surfaces of these two landslides did not form near or along the contact but developed higher into the *Qglv* unit, where higher pore pressures were measured.

The multi-year records of available piezometer data collected post-event for first-time landslides propagating deeply within intact *Qglv* deposits indicate no discernible response to heavy, short-duration (days to weeks) precipitation or rain-on-snow events. Yet, a circumstantial link of short-duration precipitation events triggering failure can be inferred for the Oso and Woodway landslides. At Woodway, the apparent pre-existence of tension cracks were deduced to be an important avenue for preceding weeks of heavy precipitation to infiltrate and adversely affect pore pressure within the slide mass (Landau, 1998; Arndt, 1999). It is not known if pore pressures increased deep within the *Qglv* unit through which the basal failure surface developed, nor is the exact location of that surface well defined at Woodway. For the Oso landslide, if failure initiated within the intact glacial sequence as we suggest, rather than the mantling landslide deposits, then the role of the preceding weeks of precipitation is not evident. It is unknown whether tension cracks had formed that could have provided an avenue for infiltration and consequent elevated pore pressures within the slide mass prior to failure at Oso.

Seasonal pressure flux measured within the *Qglv* units at the three instrumented landslides ranged from a few tenths of a meter to 1.5 m, peaking toward the latter half of the wet season. The Oso and BA6S piezometers show a gradual head increase over the multi-year record. Due to the well-reputed stability of vibrating wire technology, we do not expect instrument drift to be the cause of this gradual pressure increase; continued monitoring may further inform this question. Given the considerable depths and high stresses around the slide surfaces, the relatively minor seasonal fluxes would have minimal effect on the stability of slide surfaces forming within the intact *Qglv* units. Our sensitivity analyses (presented in Section 5) for the Oso and Woodway landslides using limit-equilibrium methods under drained conditions confirmed that their seasonal pressure fluxes have negligible effects on stability. It is possible, however, that a late winter pressure peak, in the range of what has been measured, could have been *"the straw that broke the camel's back"* at Oso for a slope teetering on instability. Other detrimental effects on stability, not measurable or observed, could also have resulted from above-normal precipitation of short, seasonal, or multi-year durations.

Unfortunately, the least well-characterized of the landslides described here, at Possession Bay on Whidbey Island, is of particular interest in that it collapsed during the dry summer season with no evident linkage to precipitation. At the least, this event strongly suggests that large first-time landslides in slopes founded on *Qglv* deposits can occur independently of water inputs due to cumulative seasonal precipitation or large storms, let alone both.

If precipitation does not generate a marked increase in pore pressure within a multi-year period to drive failure within intact *Qglv* deposits, then what other factors and processes might have a greater influence on slope instability?

5. Role of Shear Strength

Many large steep slopes in the Puget Lowland where *Qglv* deposits are present have exhibited long-term global stability on the order of decades to centuries. The initiation of deep-seated, first-time landslides within these deposits, including those that are the subject of this study, seem to occur well after the originating slopes formed. This observed geomorphic process of initial stability of these slopes followed after some lengthy period of time by rapid failure aligns with the long-recognized mode of progressive failure exhibited by natural and excavated slopes composed of overconsolidated silts and clays (i.e., Terzaghi, 1936; Skempton, 1964; Bjerrum, 1967). Following exhumation of the slope and the development of shear stresses, peak strength is lost through a gradual process of localized micro-cracking, crack linkage, dilation and material softening. Shear stress is progressively transferred to adjacent areas, and through this strain-softening process, an incipient surface of failure is formed through minor strain. Bjerrum (1967) stated that, *"… in the stiffer clays the rate* [of strain softening] *can be so small that the delay of a slide may be on the order of centuries.*" Given the typically slow rates observed, drained conditions likely persist through this strain-softening process.

From the onset of failure, the strength loss is precipitous and considerable. Through a long-term creep test of intact overconsolidated clay using pore-pressure reinflation, Carey and Petley (2014) documented such catastrophic failure nearly 3 months after the last increase in stress state. Further, the failure envelope from the long-term creep test fell below the envelope generated with conventional, short-term drained testing of intact samples. Catastrophic failure ensues not at peak strength, but more likely near a fully-softened state under rapidly developing undrained conditions.

We assess the pre-failure stability of three landslides under drained conditions using the Morgenstern-Price (1965) limit-equilibrium method with the SLOPE/W 2018 software (Geoslope, 2018), applying the peak anisotropic (bedding-parallel and bedding-perpendicular) and fully softened shear strengths of *Qglv* deposits presented in Table 3. For anisotropic strength, the software discretizes the horizontal and vertical components based on the orientation of the slide surface for each slice (gently inclined surfaces activate mostly horizontal strength while steep surfaces activate mostly vertical strength).

5.1 Oso Landslide

Figure 7 serves as the subsurface model for back-analysis of the 2014 landslide event. Figure 11 presents an average pressure head distribution estimated from the 3 to 4-year record of continuous pore pressure measurements used for stability analyses; the contours were estimated in the slope stability analysis software (SLOPE/W) through kriging of data from several dozen piezometers and hydrogeologic interpretation. Figure 12 shows the slope model used for analysis; the failure surface depicted is a very close approximation of its actual configuration determined from nine borings. Peak anisotropic and fully softened strengths yielded factors of safety of 1.15 and 1.00, respectively. These calculated safety factors were achieved without assuming the prior movement of landslide debris that mantled the hillslope, the process which has been inferred by previous studies.

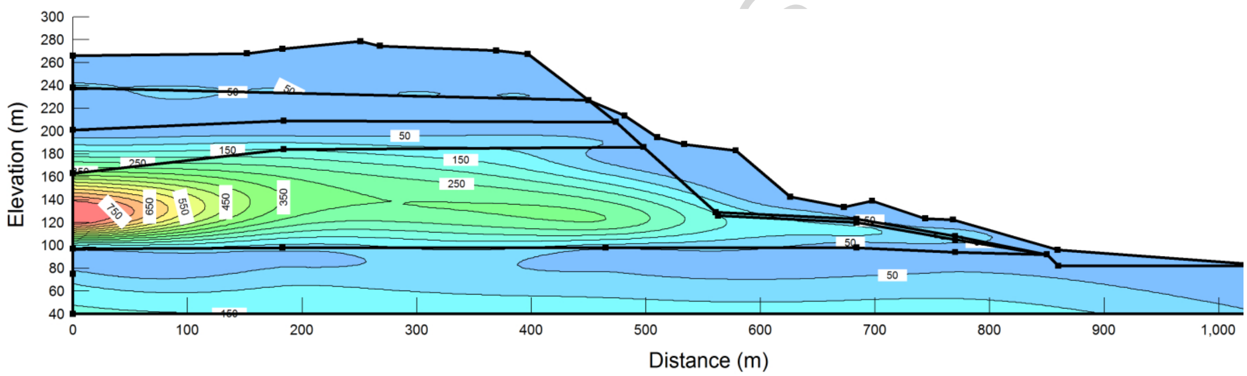

Figure 11. Estimated pressure head distribution, 50 kPa contours for the Oso landslide. (color)

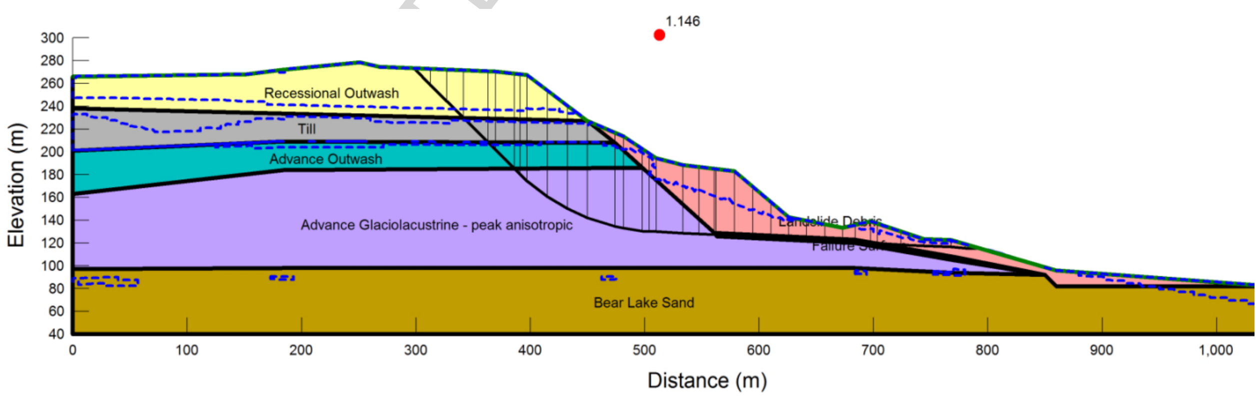

Figure 12. Calculated pre-failure stability for the Oso landslide surface using peak anisotropic strengths and pore pressure grid depicted in Figure 11. Dashed blue lines indicate piezometric surfaces or saturated zones. Red dot depicts center of rotation and respective safety factor. (color)

We performed sensitivity analyses on cohesion and friction, both parallel and perpendicular to bedding, to evaluate the influence anisotropy and the progressive loss of strength might have on stability. Strength parallel to bedding had substantially greater control on stability than strength mobilized perpendicular to bedding (Fig. 13).

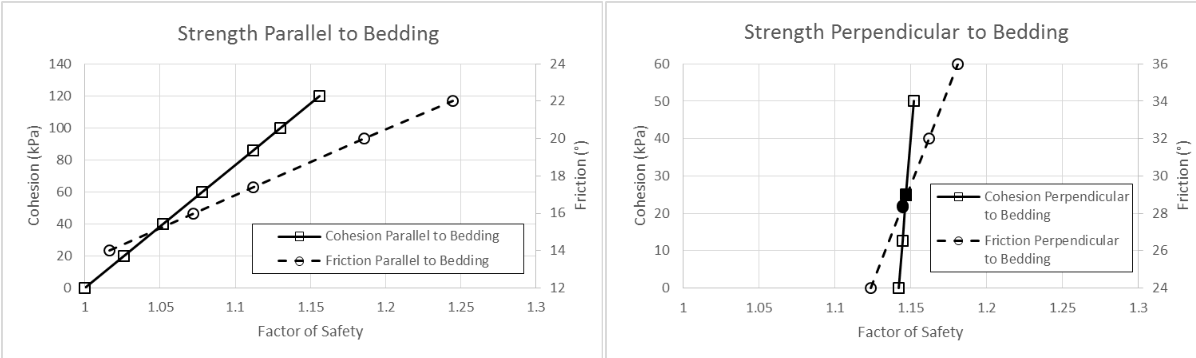

Figure 13. Sensitivity of factor of safety to strength parameters (a) parallel (φ_p=17.4° and c=86 kPa) and (b) perpendicular (φ_p=28.4° and c=12.6 kPa) to bedding.

5.2 BA6S Landslide

Under a static state, stability calculations for a single large event, as interpreted from the morphology of this landslide, could not achieve failure within a reasonable range of strengths established from laboratory testing or regional experience with these deposits and under nearly fully saturated conditions. (There was no evidence from the drilling of a confined pressurized aquifer beneath or within the failure surface.) The calculated factors of safety for the interpreted failure surface exceed 1.4 at peak strength and approach 1.2 for fully softened strengths. The calculated results suggest that either failure occurred as several smaller landslides, which is not apparent in the morphology, or that external loading (i.e., earthquake, remnant ice surcharge) played a role. Seismic sources include a proximal shallow fault zone (Darrington-Devils Mountain) and the more distal Cascadia Subduction zone, all of which have been active in the Holocene (Dragovich et al., 2003: Sherrod et al., 2008; Goldfinger et al., 2012; Personius et al., 2014). Instability of the entire mass can be achieved under modest horizontal acceleration of 0.15g and peak anisotropic strength. Horizontal acceleration can greatly lengthen the basal slide surface, even in relatively strong materials (Badger and Watters, 2004).

5.3 Woodway Landslide

We applied the peak anisotropic strengths for the *Qglv* deposits derived from the Oso landslide investigation and adopted strengths used by Savage et al. (2000b) for the other units for the geologic section depicted in Figure 5. Using similar groundwater conditions as Savage et al. (2000b) resulted in a factor of safety of 1.08 for the observed configuration of the slide surface. Stability dropped precipitously with the hypothetical reduction in cohesion.

5.4 Discussion

Given the varied sediment provenance, mixing during glacial transport and large depositional area, we have assumed for our stability calculations that material properties of *Qglv* deposits throughout the region fall within the range of values measured from the available laboratory testing and back-analyses. The extent of overconsolidation and disturbance from ice loading undoubtedly varies throughout a particular site and the region, and both factors affect strength.

The back-analyses using the peak anisotropic and fully softened strengths for intact *Qglv* deposits and measured pore pressure regimes closely replicated the observed configuration of the failure surface of the Oso landslide. Because the fully softened testing uses remolded material, the reported test results likely are higher than field conditions for horizontal shearing, due to the preservation of bedding structure in natural slopes. Additionally, the modeled stability at peak anisotropic strength yielded a state of marginal stability, and failure was achieved using a fully softened strength value. Similar states of stability were calculated for the Woodway landslide, applying the strengths derived for the Oso landslide. These results conform to our hypothesis that slopes founded on *Qglv* deposits are stable, albeit marginally, when near-peak anisotropic strength conditions exist, and that the peak anisotropic strengths established from direct shear tests reasonably approximate field conditions. Further, the long-understood behavior of time-dependent strength loss in overconsolidated silts and clays produces instability for the measured range of fully softened strength. Strength loss is thought to occur primarily through the loss of cohesion, based on comparable frictional strengths of peak and fully softened test results.

Anisotropy also exerts control on the planar and gently dipping configurations of the basal failure surfaces for the three large landslides in the North Fork Stillaguamish valley for which subsurface drilling information is available – Oso, BA6S, and BA4S (Skaglund Hill) landslides (Badger, 2015, 2016). (Subsurface information does not exist within the slide masses of the Woodway, Possession Bay and Brownsville landslides that would define the actual configurations of the basal failure surfaces.) Arcuate basal failure surfaces in these anisotropic deposits would realize more influence from higher bedding-perpendicular strength and are less critical (more stable) than planar surfaces primarily affected by lower bedding-parallel strength. The anisotropic strengths derived from the direct shear tests and used in our analyses could greatly benefit from additional testing and verification from different locations, though several studies (Giraud et al. 1991; Cruden et al., 1997; Florkiewicz et al., 2015) in other regions have also noted considerably higher strength across bedding when compared to tests conducted parallel to bedding for similar deposits.

Back-analysis for the BA6S landslide was unable to simulate failure for a single large-volume event, as seems apparent in the morphology of the slide deposit. Whether or not this landslide occurred as one large event or several smaller movements occurring in quick succession, it raises the possibility for different sources of landslide causation and landslide development. Retrospective studies that seek to establish recurrence rates, which are a necessary component of hazard and risk assessment, should consider the potential for multiple sources of causation and development.

Another potentially destabilizing factor that has not yet been discussed is toe erosion. Toe erosion from river and coastal processes within the preceding decades were not destabilizing factors at either the Oso (Pyles et al., 2016) or Woodway landslides; the pre-failure proximity of the river to the base of the slope for the prehistoric BA6S landslide is unknown.

6. Role of Stress State

The stress state along the basal slide surface directly relates to the sequence thickness of the slide mass. Basal slide surfaces of large-volume landslides in the North Fork Stillaguamish valley lie near the base of the Vashon sediment stack and the valley floor (Gerstel and Badger, 2014), involving a thickness of about 180 m. Thicknesses of the coastal landslides in this study range between about 35 and 70 m, and basal slide surfaces develop near the base of the *Qglv* deposits in those, as well.

When present within Vashon glacial deposits, *Qglv* deposits compose the base of the sequence. Commonly, they are overlain by advance outwash and tills; recessional deposits may cap this sequence. To examine the influence stress state has on stability we performed sensitivity analyses for a hypothetical sediment stack over a range of equal thicknesses of outwash and *Qglv* deposits at peak anisotropic strength. We assumed saturated conditions in the *Qglv* deposits with an overlying perched aquifer in the advance outwash deposits. We then calculated the lowest factor of safety for a slide mass with an aspect ratio (base width W / sequence thickness H) of ~0.4 to 0.6, which is characteristic for all but one of the studied slide masses, BA6S. As would be expected, stability drops with increasing total thickness (slope height), but with greater sensitivity for sequences thinner than 100 meters (Fig. 14).

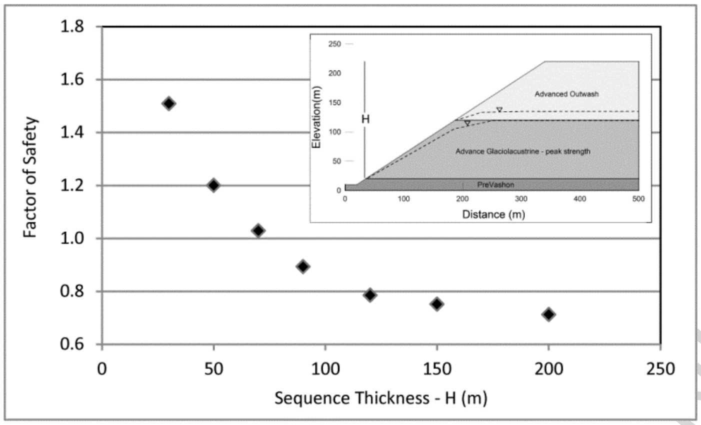

Figure 14. Relationship of slope height and factor of safety for a hypothetical two-unit section of outwash overlying mostly saturated, glaciolacustrine deposits using peak anisotropic strength.

From the interpreted geologic sections through all of the studied landslides, slide masses have the appearance of being crudely shaped parallelograms. We measured the slide mass dimensions from the interpreted sections of Arndt (1999) for the Possession Bay and Brownsville landslides, Landau Assoc. (1998) for the Woodway landslide, and Badger (2015, 2016) for the Oso and BA6S landslides. Figure 15 plots the relationship of aspect ratio with cross-sectional area, as a 2-dimensional representation of landslide volume. The data suggest that increasing sequence thickness generates proportionally greater base widths, resulting in higher aspect ratios with larger cross sectional areas. Such a relationship might be induced by proportionally greater shear stresses and lower effective stress associated with increasing stratigraphic and saturation thickness. The BA6S landslide is an obvious outlier. Perhaps not coincidentally, back-analyses of this landslide were unable to simulate static instability within a reasonable range of fully softened or residual strengths under near-fully saturated conditions, suggesting an external load on stability might have been necessary to mobilize this landslide or that it developed as two or more smaller landslides occurring in quick succession.

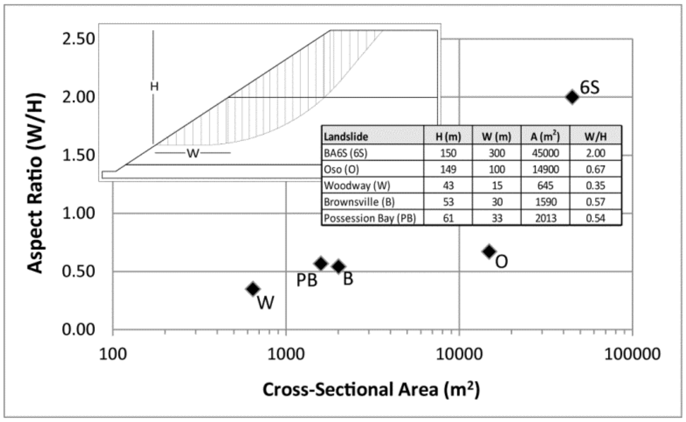

Figure 15. Relationship of aspect ratio (base width/height above failure surface) to cross-sectional area for the five studied landslides.

6.1 Discussion

The small number of first-time landslides in *Qglv* deposits for which some geomorphic and geotechnical characterization has been performed limits the robustness of the apparent relationships associated with slide mass dimensions. Considerably more data from other landslides are needed to define, refine or dispel these geomorphic inferences, in order to potentially be able to use these in a predictive manner for hazard and risk assessment. Interpretations of prehistoric landslides are shadowed with uncertainty regarding causation, singularity or multiplicity of movement events, and subsequent weathering processes. Additional sources of data from landslides in geotechnically similar glacial and nonglacial deposits, within and outside the Pacific Northwest, would prove useful to further investigate these geomorphic relations.

7. Conclusions and Application

Advance glaciolacustrine (*Qglv*) deposits from the most recent continental glaciation are widespread in the Puget Lowland, and, like similar deposits in Western Canada and Central Europe, are prone to deep-seated landsliding. Once exhumed since early postglacial time, slopes that are substantially founded on these deposits have commonly demonstrated long-term stability. Decades to centuries to millennia later, first-time landslides occur that have exhibited moderate to high mobility.

Direct shear tests performed parallel and perpendicular to bedding indicate *Qglv* strength is anisotropic: cohesion is a significant component of bedding-parallel strength whereas friction dominates strength perpendicular to bedding. Hydraulic conductivity is likely also anisotropic, with the ratio of horizontal to vertical conductivity estimated to be around two or more orders of magnitude.

Measured pore pressures within *Qglv* deposits show at most small seasonal fluxes, which peak at the end of the wet season. Only minor pore-pressure responses to multi-day to multi-week episodes of heavy precipitation and/or snowmelt have been detected, implying that these short-duration episodes do not directly reduce stability within intact *Qglv* deposits. The low and contrasting horizontal and vertical hydraulic conductivities support this conclusion, as well: short-term water inputs do not move deep into the subsurface rapidly enough to weaken these slopes. In addition, the Possession Bay landslide, having occurred during the dry season, indicates that factors other than water can be important in triggering movement in these slopes.

The pattern of long-term stability followed by abrupt collapse corresponds to the behavior of overconsolidated silts and clays of time-dependent strength loss and progressive failure. Back-analyses using limit-equilibrium methods and peak anisotropic strength under drained conditions demonstrate initial stability of the slopes; failure is calculated near the fully softened strength. Over the long term, loss of cohesive strength, rather than hydroclimatic pore pressure response, is the more important contributor to diminishing stability and, in some cases, initiation of first-time landslides in *Qglv* deposits. Given this time-dependent behavior and the relatively small strains at which abrupt strength loss ensues, useful prediction of where and when new failures might occur seems unlikely. The preexistence of tension cracks in overlying strata and fractures within *Qglv* deposits themselves would substantially increase the role precipitation could have on elevated pore pressures and landslide initiation. If such discontinuities could be observed in a slope, they might foretell imminent failure.

The shape and location of slide surfaces in these deposits is strongly influenced by strength anisotropy and stress state. Surfaces developed near the basal contact of the *Qglv* deposits in all of the study landslides. For the thickest *Qglv* deposits, located in the North Fork Stillaguamish valley, the basal slide surfaces were planar and gently dipping valley-ward sub-parallel to bedding. Analyses showed planar basal slide surfaces to be more critical (less stable) than arcuate surfaces, which are more affected by bedding-parallel than by bedding-perpendicular strengths, respectively. Higher stress states associated with increasing sequence thickness of potential landslide masses also promote instability. The length of the basal slide surface, and thus the aspect ratio of the landslide mass, appears to increase proportionally with thickness of the landslide mass.

Engineering assessment of potential deep-seated, first-time instability in these deposits would ideally consider 1) activity and nature of both historic and prehistoric instability of adjacent slopes; 2) borings within the potentially unstable mass with continuous sampling or coring and possibly cone penetration testing to confirm stratigraphy above, within and below these deposits; 3) continuous precipitation and pore pressure monitoring, especially near the base of these deposits; and 4) laboratory testing of peak and post-peak regions, emphasizing anisotropy and creep behavior. Challenges for subsurface investigations would be to identify and establish the continuity, orientation and strength of weakened zones. While short-term stability might be achieved using peak strength, long-term slope performance of natural and engineered slopes would consider post-peak strength. As an example, the Washington State Department of Transportation recommends the use of residual strength for design of permanent excavations in these deposits (WSDOT, 2018).

These findings challenge the often-inferred relationship of hydroclimatic input, pore pressure response and landslide initiation as it relate in this case to intact Vashon advance glaciolacustrine deposits, and may have relevance for similar deposits prevalent in the Northern Hemisphere. More in-depth assessment of creep behavior of these deposits and evaluation of stress state would benefit future hazard and risk assessment.

Acknowledgments

Our research and manuscript preparation were greatly aided by Ben Arndt, Rex Baum, Stan Boyle, Matt Brunengo, Trevor Contreras, Wendy Gerstel, Bob Grandorff, Kjell Karlsrud, Bill

Laprade, Erik Mikkelsen, Marv Pyles, Rick Smith, Anders Solheim and an anonymous reviewer. We also thank GeoSlope for providing the analytical software used in our work.

References

Armstrong, J.E., D.R. Crandell, D.J. Easterbrook, and J.B. Noble, 1965, Late Pleistocene stratigraphy and chronology in southwestern British Columbia and northwestern Washington, Geological Society of America Bulletin v. 76, pp. 321-330.

Arndt, B.P, 1999, Determination of the conditions necessary for slope failure of a deep-seated landslide at Woodway, Washington, M.S. thesis, Colorado School of Mines, 223 p.

Badger, T.C., 2015, SR 530 MP 35 to 41 geotechnical study, Washington State Department of Transportation, 198 p

Badger, T.C., 2016, SR 530 landslide: geotechnical data report, Washington State Department of Transportation, 355 p.
http://www.wsdot.wa.gov/publications/fulltext/Projects/SR530/SR530MP35to41GeotechnicalStudy.pdf

Badger, T.C. and R.J. Watters, 2004, Gigantic seismogenic landslides of Summer Lake basin, south-central Oregon, Geological Society of America Bulletin, v. 116, pp. 687-697.

Benda, L.E., Thorsen, G.W., Bernath, S. C., 1988, Report of the I.D. team--Investigation of the Hazel landslide on the North Fork of the Stillaguamish River (F.P.A. 19-09420), unpublished report for the Washington Department of Natural Resources, 12 p.

Bjerrum, L., 1967, Progressive failure in slopes of overconsolidated plastic clays and clay shales; Terzaghi Lecture, Journal of the Soil Mechanics and Foundations Division, American Society of Civil Engineers 93, pp. 3-49.

Booth, D.B., 1994, Glaciofluvial infilling and scour of the Puget Lowland, Washington, during ice-sheet glaciation: Geology 22.695-698

Carey, J.M. and D.N. Petley, 2014, Progressive shear-surface development in cohesive materials; implications for landslide behavior, Engineering Geology 177, pp. 54-65.
http://dx.doi.org/10.1016/j.enggeo.2014.05.009

Cooper Testing Laboratory, 2016, unpublished soil testing results, prepared for the Washington Office of the Attorney General.

Cruden, D.M., Z-Y Lu, and S. Thomson, 1997, The 1939 Matagneuse River Landslide, Alberta, Canadian Geotechnical Journal, pp. 799-810.

Dragovich, J.D., B.W. Stanton, W.S. Lingley, Jr., G.A. Griesel, and M. Polenz, 2003, Geologic map of the Mount Higgins 7.5-minute quadrangle, Skagit and Snohomish Counties, Washington, Washington Division of Geology and Earth Resources Open-File Report 2003-12, 1 sheet.

Florkiewicz, A., M. Flieger-Szymańska, K. Machowiak, and D. Wanatowski, 2015, Engineering properties of varved clays from the Junikowski Strean Valley in Poland, Geotechnics for Catastrophic Flooding Events, Taylor and Francis Group, London, pp. 267-273.

Galster, R.W. and W.T. Laprade, 1991, Geology of Seattle, Washington, United States of America, Bulletin of the Association of Engineering Geologists, pp. 235-302.

Gault, A.M., 2015, The mineralogy and strength characteristics of selected glaciolacustrine clays in the Puget Sound Region, unpublished report, University of Washington, 60 p.

Geoslope, 2018, Slope/W version 9.0.0,15234.

GeoTesting Express, 2016, unpublished soil testing results, prepared for the Washington Office of the Attorney General.

Gerstel, W.J. and T.C. Badger, 2014, Reconnaissance mapping and characterization of landslides along State Route 530 between mileposts 35 and 41, Snohomish County, Washington, report to Washington Department of Transportation Geotechnical Office, dated December 2014, 22p. http://www.wsdot.wa.gov/publications/fulltext/Projects/SR530/SR530MP35to41GeotechnicalStudy.pdf

Gerstel, W.J, M.J. Brunengo, W.S, Lingley, Jr., R.L. Logan, H. Shipman, and T.J. Walsh, 1997, Puget Sound Bluffs: the where, why and when of landslides following the 1996/97 storms, Washington Geology v. 25, pp. 17-31.

Giraud, A., P. Antoine, T.W.J. Van Asch, and J.D. Nieuwenhuis, 1991, Geotechnical problems caused by glaciolacustrine clays in the French Alps, Engineering Geology 31, pp. 185-195.

Goldfinger, C. C.H. Nelson, A.E. Morey, J.E. Johnson, J.R. Patton, E. Karabanov, J. Gutiérrez-Pastor, A.T. Eriksson, E. Gràcia, G. Dunhill, RJ. Enkin, A. Dallimore, and T.Vallier, 2012, Turbidite event history—methods and implications for Holocene paleoseismicity of the Cascadia Subduction Zone, U.S. Geological Survey Professional Paper 1661-F, 184 pp.

Henn, B., Q. Cao, D.P. Lettenmaier, C.S. Magirl, C. Mass, J.B. Bower, M. St. Laurent, Y. Mao, and S. Perica, 2015, Hydroclimatic conditions preceding the March 2014 Oso landslide, Journal of Hydrometeorology 16, pp. 1243-1249.

Hibert, C., C.P. Stark, and G. Ekström, 2014, Seismology of the Oso-Steelhead landslide, Natural Hazards and Earth System Sciences Discussions 2, pp. 7309-7327.

Holtz, R.D., W.D. Kovacs, and T.C. Sheahan, 2011, *An Introduction to Geotechnical Engineering*, 2nd edition, Prentice Hall.

Hungr, O., S. Leroueil, and L. Picarelli, 2014, The Varnes classification of landslide types, an update, Landslides, 11, pp. 167-194. doi 10.1007/s10346-013-0436-y

Iverson, R.M., D.L. George, K. Allstadt, M.E. Reid, B.D. Collins, J.W. Vallance, S.P. Schilling, J.W. Godt, C.M. Cannon, C.S. Magirl, R.L. Baum, J.A. Coe, W.H. Schultz, and J.B. Bower, 2015, Landslide mobility and hazards: implications of the 2014 Oso disaster, Earth and Planetary Science Letters 412, pp. 197-208.

Keaton, J. R., J. Wartman, S. Anderson, J. Benoit, 2014, J. deLaChapelle, R. Gilbert, and D.R. Montgomery, 2014, The 22 March 2014 Oso Landslide, Snohomish County, Washington, Geotechnical Extreme Events Reconnaissance (GEER), 186 p.

La Meil, G., 2017, Characterization of a landslide-prone glaciolacustrine clay from the Thompson River Valley near Ashcroft, British Columbia, unpublished M.S. thesis, University of Alberta, 182 p.

Landau Associates, 1998, Geotechnical engineering services Woodway Landslide Dominican Reflection Center Woodway, Washington, prepared for Dominican Sisters of Edmonds, 76 p.

Laprade, W.T., 1982, Geologic implications of pre-consolidated pressure values, Lawton Clay, Seattle, Washington, unpublished report, 20 p.

Laprade, W.T., W. Gilbert, and W.A. Hultman, 1998, Woodway landslide – a reminder and an opportunity, in, Landslides in the Puget Sound Region, ASCE seminar, 11 p.

Miller, D. J.; Miller, L. R., 1999, Hazel/Gold Basin landslides: Geomorphic review draft report: M2 Environmental Services on behalf of the US Army Corps of Engineers, 25 p.

Minard, J.P. 1982, Distribution and description of geologic units in the Mukilteo Quadrangle, Washington, U.S.G.S. Miscellaneous Field Studies Map 1438.

Morgan, D.S. and J.L. Jones, 1995, Numerical model analysis of the effects of groundwater withdrawals on discharge to streams and springs in small basins typical of Puget Sound Lowland, Washington, USGS Water Supply Paper W 2492, 73 p.

Morgenstern, N.R. and V.E. Price, 1965, The analysis of the stability of general slip surfaces, Géotechnique 15(1), pp. 79-93.
Mullineaux, D.R., H.H. Waldron, and M. Rubin, 1965, Stratigraphy and chronology of late interglacial and early Vashon glacial time in Seattle area, Washington, U.S. Geological Survey Bulletin 1194-0, 14 p.
Nieuwenhuis, J.D. and P.M.B. Van Genuchten, 1986, Feasibility of highway crossing through landslide area on varved clays, Proceedings IAEG Congress 5th, Balkema, Rotterdam, pp. 1705-1712.
Palladino, D.J. and R.B. Peck, 1972, Slope failures in an overconsolidated clay, Seattle, Washington, Géotechnique 22, pp. 563-595.
Perkins, J.P., M.E., Reid, and K.M. Schmidt, 2017, Control of landslide volume and hazard by glacial stratigraphic architecture, northwest Washington State, USA, Geology 45 (12), pp. 1139-1142.
Personius, S.F., R.W. Briggs, A.R. Nelson, E.R. Schermer, J.Z. Maharrey, B.L. Sherrod, S.A. Spaulding, and L.A. Bradley, 2014, Holocene earthquakes and right-lateral slip on the left-lateral Darrington–Devils Mountain fault zone, northern Puget Sound, Washington, Geosphere, 10(6), 1482–1500, doi:10.1130/ges01067.1.
Porter, S. C and T.W. Swanson, 1998, Radiocarbon age constraints on rates of advance and retreat of the Puget Lobe of the Cordilleran Ice Sheet during the last glaciation, Quaternary Research 50, pp. 205-213.
Pyles, M.R., J.D. Rogers, J.D. Bray, A. Skaugset, R. Storesund, and G. Schlieder, 2016, Expert opinion report (SR 530 landslide), prepared for Washington State Attorney General Office, 295 p.
Riemer, M.F., B.D. Collins, T.C. Badger, C. Toth, and Y.C. Yu, 2015, Geotechnical Soil Characterization of Intact Quaternary Deposits Forming the March 22, 2014 SR-530 (Oso) Landslide, Snohomish County, Washington, U.S. Geological Survey Open-File Report 2015-1089, 25 p.
Riemer, M.F., 2016, unpublished soil testing results, prepared for the Washington Office of the Attorney General.
Savage, W.Z, M.M. Morrisey, and R.L. Baum, 2000a, Geotechnical properties for landslide-prone Seattle-area glacial deposits, U.S. Geological Survey Open-File Report 00-28, 6 p.
Savage, W.Z., R.L. Baum, M.M. Morrissey, and B.P. Arndt, 2000b, Finite-element analysis of the Woodway landslide, Washington, U.S. Geological Survey Bulletin 218, 13 p.
Shannon, W.D., 1952, Report on slide on North Fork Stillaguamish River near Hazel, Washington: William D. Shannon and Associates [under contract to Washington Department of Game and Washington Department of Fisheries], 27 p., 7 plates.
Sherrod, B.L., R.J. Blakely, C.S. Weaver, H.M. Kelsey, E. Barnett, L. Liberty, K.L. Meagher, and K. Pape, 2008, Finding concealed active faults: extending the southern Whidbey Island fault across the Puget Lowland, Washington, Journal of Geophysical Research, 113, B05313, doi:10.1029/2007JB005060.
Skempton, A.W., 1964, Long-term stability of clay slopes; 4th Rankine Lecture, Géotechnique 14, pp. 77-102.
Skempton, A.W. and J.N. Hutchinson, 1969, Stability of natural slopes, Proceedings, 7th International Conference on Soil Mechanics, Mexico, Vol. 3, pp.291-340.
Stillaguamish Tribe, 2006, Oso Slide and North Fork Stillaguamish River Avulsion, http://www.stillaguamish.nsn.us/steelhead%20haven%20slide.htm ; accessed 3/29/2105.

Stark, T.D., A.K. Baghdady, O. Hungr, and J. Aaron, 2017, Case Study: Oso, Washington, Landslide of March 22, 2014 – material properties and failure mechanism, Journal of Geotechnical and Geoenvironmental Engineering, 143(5), [05017001]. DOI: 1061/(ASCE)GT.1943-5606.0001615.
Terzaghi, K., 1936, Stability of slopes of natural clay, Proceedings, International Conference on Soil Mechanics and Foundation Engineering, Cambridge, Massachusetts, Vol. 1, pp.161-165.
Thorsen, G. W., 1970, Landslide of January 1967 which diverted the North Fork of the Stillaguamish River near Hazel [internal memo]: Washington Division of Mines and Geology unpublished report, 8 p.
Thorson, R.M., 1980, Isostatic effects of the last glaciation in the Puget Lowland, Washington, U.S. Geological Survey Open-File Report 81-370, 110 p.
Tubbs, D.W., 1975, Causes, mechanisms and prediction of landsliding in Seattle, unpublished Ph.D. thesis, University of Washington, 88 p.
U.S. Geological Survey, Landslide Hazards Program, 2006, Precipitation, Pore-pressure, and Extensometer Measurements from area above the 1997 Woodway landslide, Snohomish County, Washington: U.S. Geological Survey, ScienceBase-Catalog, https://doi.org/10.5066/F7FB515N.
Wartman, J., D.R. Montgomery, S.A. Anderson, J.R. Keaton, J. Benoît., J. deLaChapelle, R. Gilbert, 2016, The 22 March 2014 Oso landslide, Washington, USA, Geomorphology 253 pp. 275–288.
Western Region Climate Center, https://wrcc.dri.edu/coopmap/, accessed 6/8/2018.
WSDOT, 2018, Geotechnical Design Manual, Washington State Department of Transportation, http://www.wsdot.wa.gov/Publications/Manuals/M46-03.htm.

Highlights

- Minor pore pressure response to storm and seasonal precipitation
- Deposits exhibit shear strength and hydraulic conductivity anisotropy
- Progressive loss of cohesion over long-term primary contributor to slope failure
- Configuration of failure surface influenced by strength anisotropy and stress state